IEEE Access
Multidisciplinary | Rapid Review | Open Access Journal

Received 14 December 2023, accepted 26 December 2023, date of publication 3 January 2024, date of current version 22 January 2024.

*Digital Object Identifier 10.1109/ACCESS.2023.3349374*

RESEARCH ARTICLE

# The Consumer-Centered Electricity Reliability Enhancement in the Standalone Generation Arena

**MARTIN ONYEKA OKOYE[1], GONZALO FARÍAS CASTRO[1], SEBASTIÁN FINGERHUTH[1], (Member, IEEE), AND JUNYOU YANG[2]**

[1]School of Electrical Engineering, Pontificia Universidad Católica de Valparaíso, Valparaíso 2147, Chile
[2]School of Electrical Engineering, Shenyang University of Technology, Shenyang 110870, China

Corresponding author: Martin Onyeka Okoye (martin.okoye@pucv.cl)

This work was supported by the Pontificia Universidad Católica de Valparaíso Research Grant.

**ABSTRACT** Standalone microgrids (MGs) and distributed generations (DGs) suffer power generation intermittencies. This leads to a frequent deficit in the supply to consumers. This is worsened by the further delay experienced in the transaction process of the generated energy. Critical loads face the greatest risk of the resulting power shortage. Using the blockchain-integrated data envelopment analysis (DEA), this paper proposes a customer-centered approach to minimizing these inherent issues. Consequently, generation capacity reliability is maximized while the energy supply latency is minimized. First, considering the varying generation reliabilities of standalone MGs, a simulation method is presented using the DEA algorithm for identifying and selecting the most reliable MG in real time for supply. That is, the microgrid with the maximum generation capacity. Next, to address MG's energy supply latency, a blockchain-integrated energy trading platform is proposed (for prosumers' DGs) to enhance the peer-to-peer electricity transaction experience. Thus, considering the inherent transaction delay in blockchain-integrated energy trading platforms, a DEA algorithm is proposed for determining and adopting the fastest blockchain transaction. Finally, an algorithm is developed to streamline the integration of the two-step enhancements. It was observed that, as the input data (efficiencies of MGs and blockchains) are changing, maximum power delivery and the fastest electricity transaction rate are achieved in the standalone generation arena at minimal cost. This addresses the characteristic supply deficits and delays, thus minimizing the risk of shedding critical loads.

**INDEX TERMS** Blockchain transaction, data envelopment analysis (DEA), efficiency assessment, linear regression, loss of load expectation (LOLE), multi-microgrid (MMG), peer-to-peer energy trading, reliability assessment, standalone distributed generations (DG).

## I. INTRODUCTION

### A. MICROGRID OPERATIONS

Due to low carbon emission, cost-effectiveness, and pollution-free generation, renewable sources are globally preferred and adopted for energy generation. The conventional operation of Microgrids (MGs) and distributed generations (DGs) ensures a seamless and adequate supply of power to consumers. To mitigate against supply interruption arising from contingencies and achieve reliability, MGs are conventionally connected to the utility (traditional) grid [1], [2]. This ensures a bi-directional exchange of energy to mutually meet individual demands. Depending on the consumption requirement of the local consumers, profit-and-cost optimization interest amongst operators, etc., MGs can be scaled up to include more MGs [3], [4], [5]. They typically operate in a collaborative fashion referred to as a multi-microgrid (MMG) system. Thus, energy is primarily exchanged amongst the MGs through local optimizations to meet the energy demands of the connected consumer loads. Secondary optimization

The associate editor coordinating the review of this manuscript and approving it for publication was Fabio Mottola.

is further initiated with the utility grid in the event of further demand which however was unobtainable via local optimization. The entire association ensures seamless power transmission in a quantity sufficient for the connected loads. MGs in some locations may however not be connected to the utility grid for certain reasons. There could be emergencies resulting in power disruption in the utility grid. For instance, in October 2017 in Puerto Rico, Americans were thrown into darkness by the Hurricane Maria disaster which resulted in a collapsed energy grid and communication system [6], [7]. During such incidences, MG operators disconnect from the utility grid and operate in islanded mode [8]. This is to ensure that the disruption effects are not extended. In this manner, resiliency is maintained in the MG. In addition, the long-distance remote site location of the MG from the utility grid and the resulting high cost of power transmission make MG operators decide to adopt the islanded operation fashion [9].

### B. RESEARCH CHALLENGES

#### 1) SUPPLY INADEQUACY

The islanded operation fashion of MGs however faces several bottlenecks. During the standalone operation of the MG as a result of its remote location, MMGs are commonly developed to meet the increasing load demands. However, due to the stochastic nature of renewable resources, the supply targets are frequently not met. Moreso, consistent growth in consumer loads over time worsens the situation. In addition, disruptions could also take place within the MG arena as a result of natural disasters and successful hacker-cyber attacks. Such attacks include false data injection (FDI), denial of service (DoS), malware, etc. For example, a massive blackout was experienced in the Ukrainian power grid in December 2015 which resulted from a hacker attack [10]. This left up to 225000 people in darkness for days. These incidences collectively degenerate to insufficient energy from renewable sources. To avert energy insufficiency, conventionally, individuals engage in private and independent renewable energy generation resulting in DGs. This is to achieve two purposes: (i) self-consumption sufficiency and (ii) profit-motivated trading. Thus, consumers engage in peer-to-peer (P2P) energy trading using a blockchain transaction platform to meet individual energy needs [11].

#### 2) ENERGY TRANSACTION LATENCY

Furthermore, some challenges are, however, encountered with the introduction of blockchain technology in the distributed energy P2P trading domain. Several blockchain platforms are set up to facilitate seamless energy transactions between consumers and prosumers. Blockchain deployment, however, depends largely on the availability and strength of the wireless connection amongst participating devices for data transmission. Thus, handling large transaction volumes under a weak wireless connection leaves high traffic in the network. This results in transaction delay (latency) [12]. In addition, it faces malicious cyber attacks from adversaries leading to additional delays [13], [14]. Furthermore, to boost a security measure against unforeseen malicious attacks in blockchains, a limit is inherently set to the block-creation time and transaction size [15]. This consequently sets a limit to the number of transactions admissible in each block. Thus, it results in transaction queues and consequently increases transaction latency [16]. Besides, the inconsistently increasing number of blockchain members (nodes) and their corresponding transaction sizes lead to further irregular transaction delays. This is because the number of miners to approve the entire initiated transaction sometimes becomes insufficient. These collectively lead to uncertainty in the transaction completion time of the initiated transactions due to unforeseen delays. The duration for which the transaction latency adversely affects the energy supply reliability is not definite. It depends on the rate at which the blockchain features (number of nodes, block size, and the corresponding transaction time ) vary as transactions progress. For instance, if the number of nodes and their corresponding transaction block sizes increase more rapidly, the rate at which the resulting transaction delay would affect the reliability would correspondingly increase and vice versa. The uncertainty in the transaction delay is a result of the combined effect of the standalone limited generations and the delay experienced in energy trading in the blockchain platform. While the supply inadequacy is borne by the undesired circumstances surrounding the standalone generation environment, the condition is further exacerbated by the transaction delay borne by the blockchain transaction technology during the trading of the available generations. Thus, how to improve the energy supply sufficiency and the blockchain transaction time (transaction duration) becomes a concern and a necessity.

### C. RESEARCH CONTRIBUTIONS

Researchers have made several achievements in energy management in the standalone distributed generation (DSG) arena. Akhtar [17] published a research finding on the power system reliability assessment. His research direction was, however, on the impact of integrating renewable energy resources into the main grid. A standalone operation of renewable distributed generators (RDG) was not considered. A predictive method of reliability assessment of the generation capacity was proposed in [18]. The generation capacity and load data of the 24-bus *IEEE reliability test system '96* were utilized to achieve this. Thus, RDGs and their standalone power intermittency issue were not considered. A consumer-centered electricity price optimization approach in the standalone RDG platform was successfully presented in [19], however, the electricity supply adequacy and an alternative cost optimization method were not in the scope. Various other forms of reliability assessment of power systems have been performed but each focuses on a different problem-solving domain.

Consumers' energy sufficiency in standalone generations remains a concern. To address the aforementioned challenges, this paper proposes consumer-centered approaches to maximizing energy supply, minimizing buying prices and delivery time, and ensuring greater penetrability of renewables. The specific contributions are as follows:

i. The power supply real-time reliability efficiency assessment is conducted for each MG in the remote location using data envelopment analysis (DEA). This is achieved by performing a reliability assessment of the individual MGs. Finally, the individual efficiencies of the obtained reliability magnitudes are quantified and ranked. The MG with the maximum efficiency is determined and selected.
ii. The transaction time efficiency assessment of the various blockchain-integrated energy transactive platforms is conducted using DEA. Consequently, each blockchain platform is classified, in real-time, based on its transaction timeliness. Targeting lower buying costs of electricity, the platform with the shortest transaction time is selected for energy transactions in each instance.
iii. Next, a streamlined integration of the two aforementioned enhancements is executed. Consequently, a method for selecting the most efficient MG and the fastest blockchain transaction platform is described and simulated. This is such that, as the input data (efficiencies of MGs and blockchains) are varying, the consumers are capable of identifying and selecting, in real-time, electricity sources with the maximum adequacy and minimum transaction time at the lowest cost.

## II. STANDALONE MICROGRID OPERATION

### A. THE RELIABILITIES OF STANDALONE MULTI-MICROGRIDS

#### 1) STANDALONE MULTI-MICROGRID ARCHITECTURE

Detached from the conventional MG architecture, a standalone MG lacks connection to the utility grid. This usually happens when MGs are remotely located at a very long distance from the utility grid, thus, the high connection cost and losses are averted. This could also happen when a connected MG is disconnected for safety from the utility grid as a result of a severe fault in the utility grid. The disconnection is always done to contribute to resiliency achievement in the MG. Such a standalone operation depends solely on the standalone generation capacity for supply adequacy. Due to the possibility of power insufficiency from a single MG, several other modular MGs are independently cited to augment the power supply to the surrounding rising loads. They can be interconnected to boost their energy delivery efficiency via a collaborative operation. An architecture of standalone MMGs is shown in Fig. 1 [20]. It includes $MG_1$, $MG_2$, and $MG_3$. Each of them contains (i) electrical loads being fed; (ii) RDGs that generate electrical energy from renewable sources; (iii) a battery energy storage system (BESS) which comprises modules of electrochemical cells arranged in parallel and series to achieve the desired voltage and current level; and (iv) controllable distributed generators (CDG), diesel generators whose output power is dispatchable.

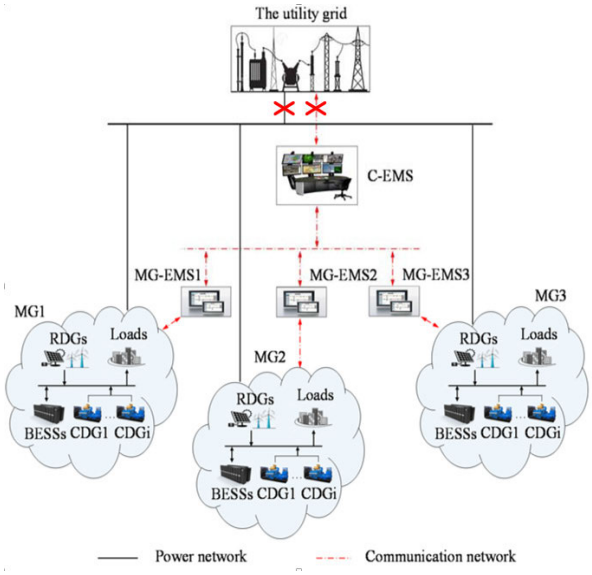


**FIGURE 1.** Standalone multi-microgrid architecture.

#### 2) STANDALONE MULTI-MICROGRID OPERATION

Local optimizations in the MGs are performed by the local energy management system (MG-EMS) [21]. Based on the magnitude of load demands, time-of-demand (ToD), and energy price at ToD, a schedule is made by MG-EMS to decide which energy generation source(s) is to be operated to minimize generation cost. For instance, during off-peak hours, the algorithm must prevent the running of the more expensive CDGs. RDGs are conventionally scheduled during the peak availability of their sources, such as, in sunny times of the day for photovoltaics (PVs) and during windy periods for wind generators. Excess energies from RDGs are stored in the BESSs. Also, during low energy prices, it schedules possible energy purchases from other MGs that have surplus generations and then stores them in the BESS. CDGs are operated during peak-demand hours when other generation sources are inadequate to supply connected loads. As a principle in the cost optimization process, sources with lower generation costs are scheduled and exhausted before those with higher costs. The central EMS (C-EMS) functions to execute optimization decisions reached by the MG-EMSs. For instance, excess energy and energy deficit from various MGs are communicated to the C-EMS for exchange. The overall aim is to collaboratively achieve cost optimizations amongst the MMGs. Also, mutual energy transactions facilitate more penetration of the generated energy thereby drawing closer to consumers' energy needs.

#### 3) STANDALONE MULTI-MICROGRID SHORTCOMINGS

Due to the daily frequent surge in the consumers' load magnitude and their consequent energy needs, the standalone RGDs frequently become incapable of meeting the consumers'

rising demands. This is due to the availability intermittency of RDG sources leading to an insufficient generation capacity. Moreso, it lacks connection to the utility grid, thus, it has no access to a regular power supply source. Thus, CDGs are frequently operated. However, similar to the demand charges, electricity prices become much higher during this time due to their inherent high operating cost. At this time, prosumers in the communities (who are consumers capable of generating energy on a smaller scale) trade their generated energy at lower prices. Sole consumers, who don't generate energy, would prefer to take advantage of prosumers' lower cost. This connects and moves prosumers and sole consumers to an energy trading platform for distributed energy transactions at lower price deals. Thus, a temporary disconnection from the MGs is made. This is however restored the moment that a lower buying price is restored. Hence, consumers characteristically seek their energy needs temporarily from the blockchain platform when the supply from MGs becomes deficit and/or when electricity cost becomes higher.

### B. DISTRIBUTED ENERGY TRANSACTIONS

#### 1) BLOCKCHAIN TRANSACTIVE TECHNOLOGY

For decentralized, convenient, cheap, and secure energy transactions, blockchain transaction technology is reliably adopted for trade between prosumers and consumers in the RDG arena. Blockchain technology improved the usual transaction fashion by moving away from the centralized trading architecture to a decentralized platform. This is as shown in Fig. 2. The conventional cost and delay bottlenecks associated with the presence of the intermediary (middleman) are thus eliminated [22]. Traditionally, transaction payments to the energy sellers were usually done through intermediaries. Thus, blockchain's intervention shortens the transaction time and lowers transaction costs that would have been incurred with the presence of an intermediary [23]. It grants direct access to every member of the consortium thereby also increasing transaction convenience.

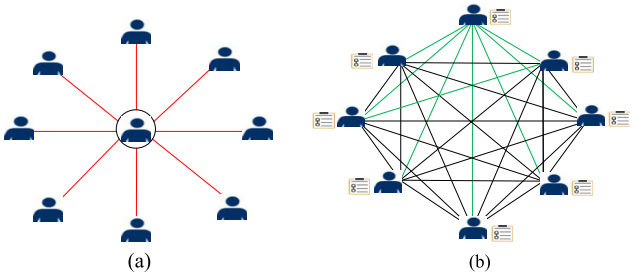


**FIGURE 2. Blockchain transaction platform (a) Centralized platform, (b) Decentralized platform.**

Another benefit of adopting blockchain technology in energy trading is its high-security feature. Each member of the consortium is known as a node. For instance, there are 8 nodes in Fig. 2 (b). Energy trading requests are made from each consumer to prosumer in sizes of bytes or kilobytes [24]. The greater the amount of energy transaction requests, the greater the corresponding data size. Usually, various transaction requests made within the same time interval are assembled into a block with a size limit and dispatched for the transaction. This block size increases with an increase in transaction requests. Each completed node-to-node (N2N) transaction is stored in a distributed ledger which is maintained by a smart contract [25], [26]. The smart contract contains every completed transaction as well as the consensus algorithm on which blockchain transactions depend [16]. The consensus algorithm is used by the smart contract to digitally execute and update members' transaction agreements. A copy of the contract is made available to every node as shown in Fig. 2 (b). Thus, each node has a record of every completed transaction on the blockchain network.

The transaction blocks are uniquely chained to one another as shown in Fig. 3. As more and more transaction blocks are completed, they are added to the existing chain, hence the unique name, blockchain. Each block is securely tied to the preceding and subsequent blocks with alphanumeric strings [27] known as hash keys [28], [29]. Each block contains two hash keys such that one hash key is tied to the immediately preceding block and the other is tied to the immediate next block [13]. Hence, for an adversary to tamper with the concatenated transaction data, he must be able to know the entire hash keys of the entire blocks in the chain. This is almost impossible. Thus, in this manner, the security of blockchain-integrated transactions is guaranteed.

#### 2) BLOCKCHAIN TECHNOLOGY SHORTCOMINGS

One of the shortcomings of blockchain transaction support is that as the number of nodes and the corresponding transactions increase, the transaction time becomes increasingly unwelcoming. The transaction time, also regarded as transaction latency, is the time it takes for an initiated energy transaction request to be completed. This delay is due to blockchain technology's dependence on certain factors. Such factors include WIFI connection strength, number of nodes, size of transaction bandwidth, etc. As the number of nodes and their consequent transaction block size grows, the transaction bandwidth reduces. This, in return, causes a decrease in transaction throughput leading to a transaction delay. Thus, transaction time increases. Also, the network miners, whose responsibility is to approve the initiated transactions, might not be able to approve the entire rising number of transaction requests. This translates to a delay in transactions that are not promptly approved. In addition, nodes with weaker device connection strength might experience a delay in their initiated transactions compared to other devices with stronger connection strength.

Furthermore, in blockchain networks, some consumers rarely engage in energy purchases. However, blockchain inherently sends all transaction data to all nodes in the network. These data, in the form of chains of transaction blocks, are multiplied as many times as the number of nodes and are stored in the network. Hence, the two issues here include high-traffic data transmission which narrows the

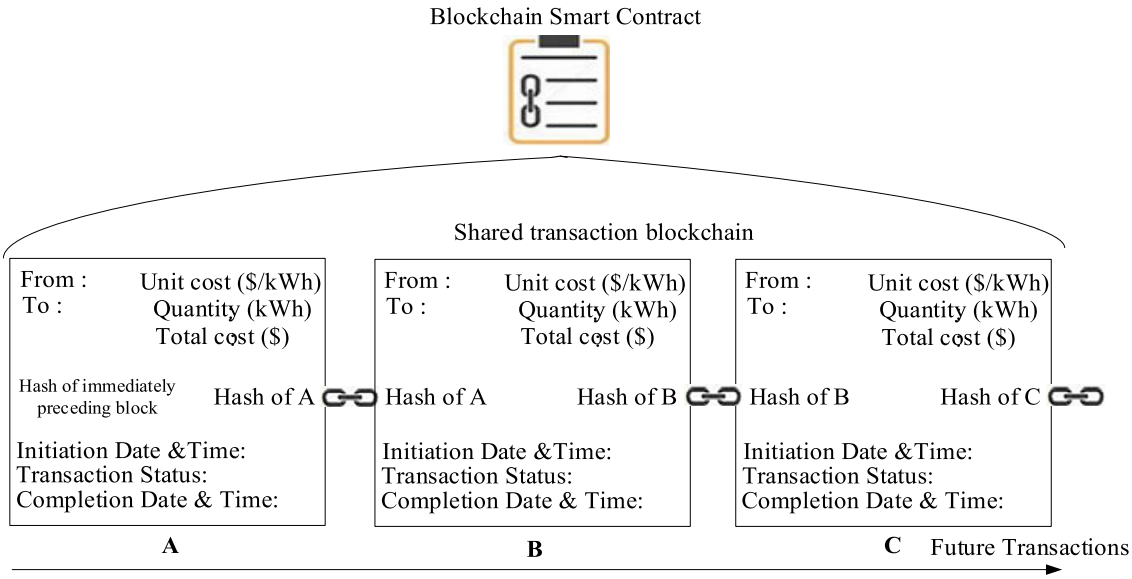


**FIGURE 3.** Secure blockchain transaction blocks.

network bandwidth and decreases transaction throughput. This consequently leads to higher transaction latency. The other issue is the high storage size occupied by the stored data. This makes blockchain applications sometimes slow in some nodes whose devices have lower device specifications, such as lower storage drive and lower RAM size. In this condition, individually initiated energy transactions might experience an undesired delay. The aforementioned transaction time delays in the blockchain transactive platform point to one reason: the increasing number of nodes and transaction block size. Therefore, energy consumers prefer individual blockchain networks whose nodes comprise prosumers and only consumers with high transaction patronage. The intent is to own a faster transaction advantage by cutting off redundant nodes. Thus, the number of nodes and corresponding block size is kept minimal. Some prosumers might, however, reach a consensus with other like-feature prosumers to collaboratively trade on the same blockchain network. This is for the advantage of energy sharing and balancing in times of surplus or insufficient generation. Thus, during peak demand, a prosumer with insufficient generation could purchase energy from counterparts whose generation is surplus and then resell it to her immediate consumers. However, consumers remain at the receiving end as their initiated transactions frequently remain delayed at their expense. Hence, a consumer-centered approach remains a solution to both the energy insufficiency within the standalone MGs as well as the delay in the blockchain transaction arena.

## III. CONSUMER-CENTERED APPROACH TO ENERGY ADEQUACY AND COST OPTIMIZATION

Following (i) the power generation intermittency and the resulting insufficiency in the standalone MG RDGs and (ii) the energy price surge during the running of CDGs, we propose an energy maximization and cost minimization approach for the consumers at the receiving end. Energy maximization is implemented in the MGs while transaction time minimization is implemented in the blockchain transactive platform.

### A. MICROGRID ENERGY SUPPLY EFFICIENCY AND OPTIMIZATION

Microgrid energy supply could be surplus or deficit (insufficient) depending on its connected load capacity. It also depends on the capacity and intermittency of its RDG sources intermittency. The purpose of energy maximization within the MMG community is to identify, in real time, the MG with the maximum generation spillover (surplus) or least supply deficit. Then, consumers can migrate under the load coverage of that MG to enjoy a minimum supply deficit at a lower cost. To identify such an MG with maximum supply efficiency, the individual reliability assessment of all MGs is conducted. Thereafter, the efficiency assessment of the obtained reliabilities is conducted. The MG that yields the maximum efficiency ranking is selected at the moment. Due to the intermittency characteristic of the RDG sources, this ranking would vary with time. At a time, the MG with the least supply efficiency could become the most efficient MG. Because standalone renewable generations are intermittent and frequently inadequate, the consumers characteristically connect to more than one MG with the intent to optimize supply and cost benefits at regular intervals through switching processes. Thus, an algorithm is developed to identify and select, in real-time, the most efficient MG at each instance. Next, an automated switch-over system dynamically switches consumers to the best-performing grid at the desired time intervals from the comfort of their homes.

### 1) RELIABILITY ASSESSMENT OF MICROGRID SUPPLY

The reliability assessment is performed to determine the period, usually in hours, during which the MG's supply is in deficit in a year (8736 hours). It could also be recorded in minutes, days, or even years as the demand warrants. Also known as the risk model, it is the period during which the consumer load magnitude surpasses the MG generation capacity. This is illustrated in Fig 4 as the summation of the two red-colored regions, x+y. The assessment is thus conducted for each of the MMGs to determine their supply reliability.

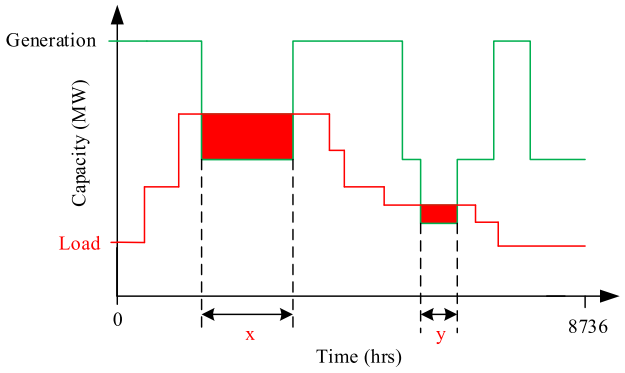


**FIGURE 4.** The risk Model.

The reliability assessment of the generation system was conducted in our paper in [18]. A reliability index, loss of load expectation (LOLE), was used to quantify the reliability strength. LOLE is the time duration for which the load magnitude exceeds the generation capacity. It is the duration of power supply deficiency. From Fig. 4, LOLE is equivalent to x+y as expressed in (1). To investigate its effect on the LOLE on the existing generation capacity, the load magnitude was gradually increased stepwise and in uniform percentages. It was found that LOLE is directly proportional to the load increment. A graph of the relationship between load increment and the corresponding LOLE recorded is given in Fig. 5. The load data and the generation capacity data that were utilized were obtained from the IEEE Reliability Test System (IEEE RTS) 1996. From Fig. 5, the linear relationship between load increment and LOLE was obtained as given in (2) using the linear regression algorithm.

$$LOLE = x + y \tag{1}$$

$$LOLE = 45.84L + 5.29 \tag{2}$$

In this paper, a similar approach is deployed to assess the reliability of each MG in the MMG arena. Consequently, two more MGs, $MG_2$ and $MG_3$, were considered and modeled using (2) as a reference equation. Hence, the equations are formulated using the ranges of LOLE and L as contained in the parent equation (2). For instance, the LOLE in equation (2) ranges from 6.16 to 1380.66 as shown in (3). Also, the load increment, L, ranges from 0 to 30% as shown in (4). Thus, for each of the L and LOLE, two streams of data are generated representing $MG_2$ and MG3 data. An uninfluenced generation and demand data sequence was upheld in

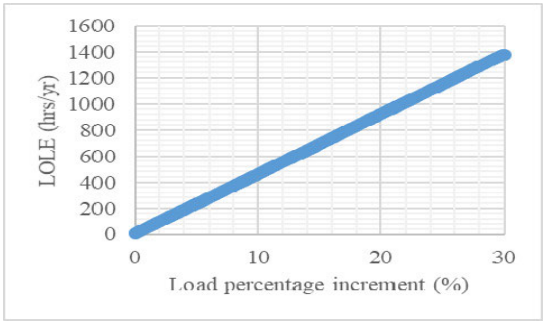


**FIGURE 5.** The load and LOLE relationship.

the microgrids' scheduling. This is to maintain fairness and uninfluenced randomness in the generation dispatch amongst the microgrids as well as the consumption history in the load. To uphold uninfluenced relationships in the generated data, a random number generator is utilized. To enable the reproducibility of our simulation work, the random numbers are seeded such that when regenerated, the same data values are obtained.

$$6.16 \leq LOLE \leq 1380.66 \tag{3}$$

$$0\% \leq L \leq 30\% \tag{4}$$

The first stream of load ($L_g$) and the corresponding LOLE ($LOLE_g$) are generated for $MG_2$ using the Python codes in Table 1 and Table 2, respectively. The subscript, g, represents the index of the MG. Line 2 seeds the random number using the value, 1. Line 3 generates the values in 15 rows which corresponds to 15 input-and-output data. The data is made up of 15 rows to be sufficient for linear regression analyses to be performed. Line 4 generates and prints the data in 2 decimal values within the specified lower and upper bounds.

**TABLE 1.** Python code for generating the Load ($L_2$) of $MG_2$.

| Line | Command |
|---|---|
| 1 | import random |
| 2 | random.seed (1) |
| 3 | for i in range (15): |
| 4 | print (round (random.uniform(0,30), 2)) |

**TABLE 2.** Python code for generating the $LOLE_2$ of $MG_2$.

| Line | Command |
|---|---|
| 1 | import random |
| 2 | random.seed (1) |
| 3 | for i in range (15): |
| 4 | print (round (random.uniform(6.16, 1380.66), 2)) |

Similarly, $L_3$ and $LOLE_3$ of $MG_3$ are obtained using the value, 2, as the random number seed. The resulting values of $L_2$ & $LOLE_2$ and $L_3$ & $LOLE_3$ for $MG_2$ and $MG_3$, respectively, are shown in Table 3. From Table 3, the relationship between $L_2$ and $LOLE_2$ is graphically shown in Fig. 6 while that of $MG_3$ is given in Fig. 7.

From Fig. 6 and Fig. 7, it was found that the relationship between load increment and LOLE is linear, hence, a linear

**TABLE 3. Load and LOLE Data for MG2 and MG3.**

| S/No | $MG_2$ | | $MG_3$ | |
|---|---|---|---|---|
| | $L_2$ (%) | $LOLE_2$ (hrs/yr) | $L_3$ (%) | $LOLE_3$ (hrs/yr) |
| 1 | 4.03 | 190.84 | 28.68 | 1320.23 |
| 2 | 25.42 | 1170.96 | 28.43 | 1308.95 |
| 3 | 22.91 | 1055.97 | 1.7 | 83.89 |
| 4 | 7.65 | 356.75 | 2.55 | 122.82 |
| 5 | 14.86 | 687.14 | 25.06 | 1154.55 |
| 6 | 13.48 | 623.99 | 22.08 | 1017.75 |
| 7 | 19.55 | 901.77 | 20.09 | 926.7 |
| 8 | 23.66 | 1090.26 | 9.24 | 429.69 |
| 9 | 2.82 | 135.17 | 18.18 | 839.03 |
| 10 | 0.85 | 45.12 | 18.2 | 840.21 |
| 11 | 25.07 | 1154.92 | 17.44 | 805.02 |
| 12 | 12.98 | 601.0 | 4.75 | 223.86 |
| 13 | 22.87 | 1053.91 | 12.92 | 598.12 |
| 14 | 0.06 | 9.05 | 11.81 | 547.07 |
| 15 | 13.36 | 618.34 | 21.69 | 999.94 |

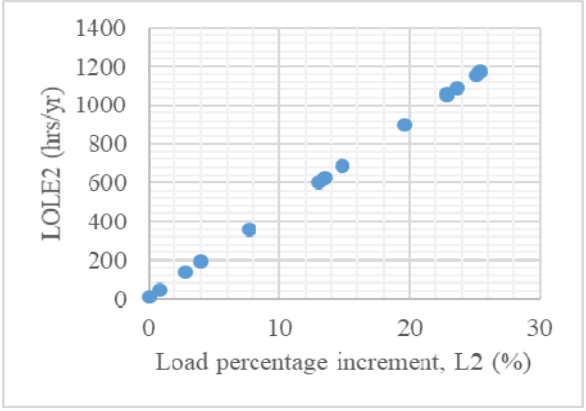


**FIGURE 6. The load and LOLE relationship for $MG_2$.**

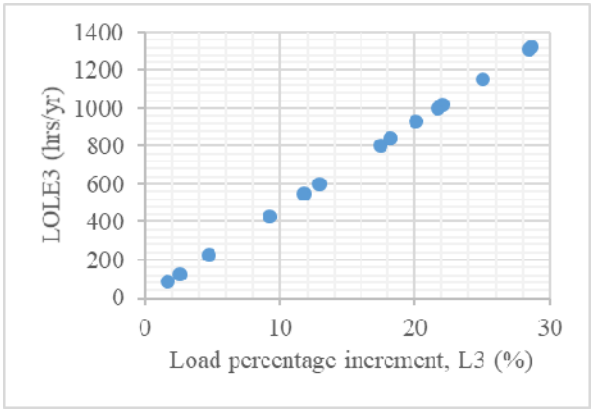


**FIGURE 7. The load and LOLE relationship for $MG_3$.**

regression algorithm was used to model the source data in Table 3. Consequently, the resulting fitting formula for $MG_2$ and $MG_3$ is given in (5) and (6), respectively.

$$LOLE_2 = 45.819L_2 + 6.1928 \tag{5}$$

$$LOLE_3 = 45.825L_3 + 6.043 \tag{6}$$

To assess and compare the reliability efficiencies of $MG_1$, $MG_2$, and $MG_3$ and determine the one with the maximum efficiency, their corresponding equations (2), (5), and (6) are optimized and compared, respectively. This is achieved using the DEA. Other optimization algorithms, such as particle swam optimization, artificial bee colony algorithm, etc could have been selected as an alternative to the DEA. However, a high precision is required for the accuracy of the optimized result. This is because the optimization involves more than one quantity (MG 1-3 and BCH 1-3). Hence, several (three) optimization results are obtained and compared. Meanwhile, their input data values have thin separation boundaries. The accuracy of a search-based heuristic algorithm, such as PSO and others, does not have such a high precision in their results. An iteration-obtained result is thus not reliable in this scenario considering the comparisons in the MGs and BCHs efficiencies. Thus, the robustness and high accuracy level of the DEA algorithm [30] made it a perfect match for the optimization purpose in our paper.

In this paper, only three MGs were considered. This is for simplicity and less ambiguity. Otherwise, more than three MGs could be cited in the remote locality depending on the magnitude of the load demand and the financial capacity of the local operators.

### 2) EFFICIENCY ASSESSMENT OF MICROGRID RELIABILITIES

The efficiency assessment of the reliabilities of $MG_1$, $MG_2$, and $MG_3$ is achieved using the DEA model. In a nutshell, the DEA is a nonparametric and robust method of comparing the efficiencies of various alternatives to an objective [31], [32], [33]. Each alternative is terminologically regarded as a decision-making unit (DMU). It is an input and output-oriented multiobjective optimization algorithm. It offers a robust approach for advanced decision-making when comparing various alternatives whose individual features do not have a clear separation for judgment during comparison. It was adopted in preference over other conventional multiobjective optimization algorithms because its algorithm accommodates multi-input and multi-output simulation data. For instance, the generation efficiency assessment and blockchain transaction time assessment have input and output data orientations. DEA specifically performs better in systems with similar input-output data orientations. DEA was first proposed by Charnes et al. in 1978 [34], [35]. Several DMUs, each with individual inputs and outputs, are compared. Thereafter, the DMU which offers the maximum efficiency is selected as the most efficient alternative for deployment.

There are two approaches to achieving the task. The input-oriented approach and output-oriented approach. In the input-oriented, the objective is to minimize the inputs given the output. The DMU whose inputs collectively yield the minimum value becomes the alternative to be selected. Similarly, in the output-oriented approach, the outputs are maximized given the existing input. The DMU whose outputs yield the maximum value becomes the alternative to be selected. Thus, in either of the two approaches, the linear

programming algorithm is used to achieve the purpose. For instance, consider alternatives with n number of DMUs as shown in Table 4. d is the index of DMUs where d = d1, d2, d3, …, dn. For example, d2 is the second DMU, d3 is the third DMU, and dn is the nth DMU. Each DMU has m number of inputs, i; and p number of outputs, o; as shown in Table 4 (a) and Table 4 (b); respectively. Thus, i = i1, i2, i3 …, im and o = o1, o2, o3, …, op.

### a: THE INPUT-ORIENTED APPROACH

The objective of the input-oriented DEA efficiency assessment approach is to minimize $\phi$ in (7) such that the constraint in (8) is achieved.

$$\sum_{d=1}^{n} (\lambda_d x_{\mathrm{d\,i}}) \leq \phi x'_{\mathrm{d\,i}} \tag{7}$$

$$\sum_{d=1}^{n} (\lambda_d y_{do}) \geq y'_{do} \tag{8}$$

where $x$ = input value of a DMU; $y$= output value of a DMU; $x_{\mathrm{d\,i}}$ = ith input of the dth DMU (i.e., the input value, $x$, at dth row and ith column); $x'_{\mathrm{d\,i}}$ = ith input of the dth DMU whose efficiency is currently being calculated; $y_{d\,o}$ = oth output of the dth DMU; $y'_{d\,o}$ = oth output of the dth DMU whose efficiency is currently being calculated; n = number of DMUs, d; $\lambda_d$ = weight of the dth DMU; and $\phi$ = efficiency of $x'_{\mathrm{d\,i}}$. Thus, the values of Table 4 (a) and Table 4 (b) are shown in Table 5 (a) and Table 5 (b), respectively. For example, from Table 5, the efficiency ($\phi_1$) of DMU1 (d1) is calculated by minimizing $\phi$ in (9) given the constraint in (10) (refer to (7) and (8)). Similarly, the efficiency ($\phi_{\mathrm{n}}$) of DMUn (dn) is calculated by minimizing $\phi$ in (11) given the constraint in (12), and so on.

Finally; $\phi_1$, $\phi_2$, $\phi_3$, …., $\phi_{\mathrm{n}}$ are obtained and sorted in ascending order. The one whose input is the most minimized becomes the alternative to be selected and deployed.

$$\mathrm{Min}(\phi)$$

$$\left.\begin{aligned}
&\lambda_{d1}x_{d1\mathrm{i}1}+\lambda_{d2}x_{d2\mathrm{i}1}+\lambda_{d3}x_{d3\mathrm{i}1}+\lambda_{dn}x_{dni1} \leq \phi\lambda_{d1}x_{d1\mathrm{i}1}\\
&\lambda_{d1}x_{d1\mathrm{i}2}+\lambda_{d2}x_{d2\mathrm{i}2}+\lambda_{d3}x_{d3\mathrm{i}2}+\lambda_{dn}x_{dni2} \leq \phi\lambda_{d1}x_{d1\mathrm{i}2}\\
&\lambda_{d1}x_{d1\mathrm{i}3}+\lambda_{d2}x_{d2\mathrm{i}3}+\lambda_{d3}x_{d3\mathrm{i}3}+\lambda_{dn}x_{dni3} \leq \phi\lambda_{d1}x_{d1\mathrm{i}3}\\
&\lambda_{d1}x_{d1\mathrm{im}}+\lambda_{d2}x_{d2\mathrm{im}}+\lambda_{d3}x_{d3\mathrm{im}}+\lambda_{dn}x_{dnim} \leq \phi\lambda_{d1}x_{d1\mathrm{im}}
\end{aligned}\right. \tag{9}$$

$$\left.\begin{aligned}
&\lambda_{d1}y_{d1\mathrm{o}1}+\lambda_{d2}y_{d2\,\mathrm{o}1}+\lambda_{d3}y_{d3\mathrm{o}1}+\lambda_{dn}y_{dno1} \geq \lambda_{d1}y_{d1\mathrm{o}1}\\
&\lambda_{d1}y_{d1\mathrm{o}2}+\lambda_{d2}y_{d2\mathrm{o}2}+\lambda_{d3}y_{d3\mathrm{o}2}+\lambda_{dn}y_{dno2} \geq \lambda_{d1}y_{d1\mathrm{o}2}\\
&\lambda_{d1}y_{d1\mathrm{o}3}+\lambda_{d2}y_{d2\mathrm{o}3}+\lambda_{d3}y_{d3\mathrm{o}3}+\lambda_{dn}y_{dno3} \geq \lambda_{d1}y_{d1\mathrm{o}3}\\
&\lambda_{d1}y_{d1\mathrm{op}}+\lambda_{d2}y_{d2\mathrm{op}}+\lambda_{d3}y_{d3\mathrm{op}}+\lambda_{dn}y_{dnop} \geq \lambda_{d1}y_{d1\mathrm{op}}
\end{aligned}\right\} \tag{10}$$

$$\mathrm{Min}(\phi)$$

$$\left.\begin{aligned}
&\lambda_{d1}x_{d1\mathrm{i}1}+\lambda_{d2}x_{d2\mathrm{i}1}+\lambda_{d3}x_{d3\mathrm{i}1}+\lambda_{dn}x_{dni1} \leq \phi\lambda_{dn}x_{dni1}\\
&\lambda_{d1}x_{d1\mathrm{i}2}+\lambda_{d2}x_{d2\mathrm{i}2}+\lambda_{d3}x_{d3\mathrm{i}2}+\lambda_{dn}x_{dni2} \leq \phi\lambda_{dn}x_{dni2}\\
&\lambda_{d1}x_{d1\mathrm{i}3}+\lambda_{d2}x_{d2\mathrm{i}3}+\lambda_{d3}x_{d3\mathrm{i}3}+\lambda_{dn}x_{dni3} \leq \phi\lambda_{dn}x_{dni3}\\
&\lambda_{d1}x_{d1\mathrm{im}}+\lambda_{d2}x_{d2\mathrm{im}}+\lambda_{d3}x_{d3\mathrm{im}}+\lambda_{dn}x_{dnim} \leq \phi\lambda_{dn}x_{dnim}
\end{aligned}\right. \tag{11}$$

**TABLE 4.** nDMUs (a) with m Inputs, (b) with p Outputs.

(a)

| | i1 | i2 | i3 | im |
|---|---|---|---|---|
| d1 | | | | |
| d2 | | | | |
| d3 | | | | |
| dn | | | | |

(b)

| | o1 | o2 | o3 | op |
|---|---|---|---|---|
| d1 | | | | |
| d2 | | | | |
| d3 | | | | |
| dn | | | | |

**TABLE 5.** Input Values of Table 4 (a), (b) Output Values of Table 4 (b).

(a)

| | i1 | i2 | i3 | im |
|---|---|---|---|---|
| d1 | $\lambda_{d1}x_{d1\,\mathrm{i}1}$ | $\lambda_{d1}x_{d1\,\mathrm{i}2}$ | $\lambda_{d1}x_{d1\,\mathrm{i}3}$ | $\lambda_{d1}x_{d1\,\mathrm{im}}$ |
| d2 | $\lambda_{d2}x_{d2\,\mathrm{i}1}$ | $\lambda_{d2}x_{d2\,\mathrm{i}2}$ | $\lambda_{d2}x_{d2\,\mathrm{i}3}$ | $\lambda_{d2}x_{d2\,\mathrm{im}}$ |
| d3 | $\lambda_{d3}x_{d3\,\mathrm{i}1}$ | $\lambda_{d3}x_{d3\,\mathrm{i}2}$ | $\lambda_{d3}x_{d3\,\mathrm{i}3}$ | $\lambda_{d3}x_{d3\,\mathrm{im}}$ |
| dn | $\lambda_{dn}x_{dn\,\mathrm{i}1}$ | $\lambda_{dn}x_{dn\,\mathrm{i}2}$ | $\lambda_{dn}x_{dn\,\mathrm{i}3}$ | $\lambda_{dn}x_{dn\,\mathrm{im}}$ |

(b)

| | o1 | o2 | o3 | op |
|---|---|---|---|---|
| d1 | $\lambda_{d1}y_{d1\,\mathrm{o}1}$ | $\lambda_{d1}y_{d1\,\mathrm{o}2}$ | $\lambda_{d1}y_{d1\,\mathrm{o}3}$ | $\lambda_{d1}y_{d1\,\mathrm{op}}$ |
| d2 | $\lambda_{d2}y_{d2\,\mathrm{o}1}$ | $\lambda_{d2}y_{d2\,\mathrm{o}2}$ | $\lambda_{d2}y_{d2\,\mathrm{o}3}$ | $\lambda_{d2}y_{d2\,\mathrm{op}}$ |
| d3 | $\lambda_{d3}y_{d3\,\mathrm{o}1}$ | $\lambda_{d3}y_{d3\,\mathrm{o}2}$ | $\lambda_{d3}y_{d3\,\mathrm{o}3}$ | $\lambda_{d3}y_{d3\,\mathrm{op}}$ |
| dn | $\lambda_{dn}y_{dn\,\mathrm{o}1}$ | $\lambda_{dn}y_{dn\,\mathrm{o}2}$ | $\lambda_{dn}y_{dn\,\mathrm{o}3}$ | $\lambda_{dn}y_{dn\,\mathrm{op}}$ |

$$\left.\begin{aligned}
&\lambda_{d1}y_{d1\mathrm{o}1}+\lambda_{d2}y_{d2\,\mathrm{o}1}+\lambda_{d3}y_{d3\mathrm{o}1}+\lambda_{dn}y_{dno1} \geq \lambda_{dn}y_{dno1}\\
&\lambda_{d1}y_{d1\mathrm{o}2}+\lambda_{d2}y_{d2\mathrm{o}2}+\lambda_{d3}y_{d3\mathrm{o}2}+\lambda_{dn}y_{dno2} \geq \lambda_{dn}y_{dno2}\\
&\lambda_{d1}y_{d1\mathrm{o}3}+\lambda_{d2}y_{d2\mathrm{o}3}+\lambda_{d3}y_{d3\mathrm{o}3}+\lambda_{dn}y_{dno3} \geq \lambda_{dn}y_{dno3}\\
&\lambda_{d1}y_{d1\mathrm{op}}+\lambda_{d2}y_{d2\mathrm{op}}+\lambda_{d3}y_{d3\mathrm{op}}+\lambda_{dn}y_{dnop} \geq \lambda_{dn}y_{dnop}
\end{aligned}\right\} \tag{12}$$

The format of the minimization equation is that the summation of the individual units (composite unit) is less than or equal to the operating unit multiplied by its efficiency. The operating unit is the unit whose efficiency is currently being calculated. From the inputs and outputs in Table 5, the format of the objective function of the minimization equation is given as:

$$\mathrm{Min}(\phi) \left|\begin{aligned}
&i1_{(composite\ unit)} &&\leq i1_{(operating\ unit)} * \phi_{(operating\ unit)}\\
&i2_{(composite\ unit)} &&\leq i2_{(operating\ unit)} * \phi_{(operating\ unit)}\\
&i3_{(composite\ unit)} &&\leq i3_{(operating\ unit)} * \phi_{(operating unit)}\\
&im_{(composite\ unit)} &&\leq im_{(operating\ unit)} * \phi_{(operating\ unit)}
\end{aligned}\right.$$

(Objective function)

The format of the minimization constraint, from Table 5, is given as:

$$\left.\begin{aligned}
&o1_{(composite\ unit)} &&\geq o1_{(operating\ unit)}\\
&o2_{(composite\ unit)} &&\geq o2_{(operating unit)}\\
&o3_{(composite\ unit)} &&\geq o3_{(operating\ unit)}\\
&\mathrm{op}_{(composite\ unit)} &&\geq \mathrm{op}_{(operating\ unit)}
\end{aligned}\right\} \text{(Constraint)}$$

*b: THE OUTPUT-ORIENTED APPROACH*

For the output-oriented model, the objective is to maximize $\theta$ in (13) such that the constraint in (14) is achieved.

$$\sum_{d=1}^{n} (\lambda_d y_{d\,o}) \geq \theta y'_{do} \tag{13}$$

$$\sum_{d=1}^{n} (\lambda_d x_{\mathrm{d\,i}}) \leq x'_{\mathrm{d\,i}} \tag{14}$$

It is important to notice that for the output-oriented approach, efficiency ($\phi$) is the inverse of $\theta$ (i.e., $\phi = 1/\theta$). For example, from Table 5, the efficiency ($\phi_1$) of DMU1 (d1) is calculated by maximizing $\theta$ in (15) given the constraint in (16) (refer to (13) and (14)). Similarly, the efficiency ($\phi_{\mathrm{n}}$) of DMUn (dn) is calculated by maximizing $\theta$ in (17) given the constraint in (18), and so on. Finally; $\phi_1$, $\phi_2$, $\phi_3$, ...., $\phi_{\mathrm{n}}$ are obtained and sorted. The one whose value is the maximum is the most efficient alternative to be selected and deployed.

$$\mathrm{Max}(\phi)$$

$$\left|\begin{array}{l}
\lambda_{d1}y_{d1\mathrm{o}1} + \lambda_{d2}y_{d2\,\mathrm{o}1} + \lambda_{d3}y_{d3\mathrm{o}1} + \lambda_{dn}y_{dn\mathrm{o}1} \geq \theta\lambda_{d1}y_{d1\mathrm{o}1} \\
\lambda_{d1}y_{d1\mathrm{o}2} + \lambda_{d2}y_{d2\mathrm{o}2} + \lambda_{d3}y_{d3\mathrm{o}2} + \lambda_{dn}y_{dn\mathrm{o}2} \geq \theta\lambda_{d1}y_{d1\mathrm{o}2} \\
\lambda_{d1}y_{d1\mathrm{o}3} + \lambda_{d2}y_{d2\mathrm{o}3} + \lambda_{d3}y_{d3\mathrm{o}3} + \lambda_{dn}y_{dn\mathrm{o}3} \geq \theta\lambda_{d1}y_{d1\mathrm{o}3} \\
\lambda_{d1}y_{d1\mathrm{op}} + \lambda_{d2}y_{d2\mathrm{op}} + \lambda_{d3}y_{d3\mathrm{op}} + \lambda_{dn}y_{dn\mathrm{op}} \geq \theta\lambda_{d1}y_{d1\mathrm{op}}
\end{array}\right. \tag{15}$$

$$\left.\begin{array}{l}
\lambda_{d1}x_{d1\mathrm{i}1} + \lambda_{d2}x_{d2\mathrm{i}1} + \lambda_{d3}x_{d3\mathrm{i}1} + \lambda_{dn}x_{dn\mathrm{i}1} \leq \lambda_{d1}x_{d1\mathrm{i}1} \\
\lambda_{d1}x_{d1\mathrm{i}2} + \lambda_{d2}x_{d2\mathrm{i}2} + \lambda_{d3}x_{d3\mathrm{i}2} + \lambda_{dn}x_{dn\mathrm{i}2} \leq \lambda_{d1}x_{d1\mathrm{i}2} \\
\lambda_{d1}x_{d1\mathrm{i}3} + \lambda_{d2}x_{d2\mathrm{i}3} + \lambda_{d3}x_{d3\mathrm{i}3} + \lambda_{dn}x_{dn\mathrm{i}3} \leq \lambda_{d1}x_{d1\mathrm{i}3} \\
\lambda_{d1}x_{d1\mathrm{im}} + \lambda_{d2}x_{d2\mathrm{im}} + \lambda_{d3}x_{d3\mathrm{im}} + \lambda_{dn}x_{dn\mathrm{im}} \leq \lambda_{d1}x_{d1\mathrm{im}}
\end{array}\right\} \tag{16}$$

$$\mathrm{Max}(\phi)$$

$$\left|\begin{array}{l}
\lambda_{d1}y_{d1\mathrm{o}1} + \lambda_{d2}y_{d2\,\mathrm{o}1} + \lambda_{d3}y_{d3\mathrm{o}1} + \lambda_{dn}y_{dn\mathrm{o}1} \geq \theta\lambda_{dn}y_{dn\mathrm{o}1} \\
\lambda_{d1}y_{d1\mathrm{o}2} + \lambda_{d2}y_{d2\mathrm{o}2} + \lambda_{d3}y_{d3\mathrm{o}2} + \lambda_{dn}y_{dn\mathrm{o}2} \geq \theta\lambda_{dn}y_{dn\mathrm{o}2} \\
\lambda_{d1}y_{d1\mathrm{o}3} + \lambda_{d2}y_{d2\mathrm{o}3} + \lambda_{d3}y_{d3\mathrm{o}3} + \lambda_{dn}y_{dn\mathrm{o}3} \geq \theta\lambda_{dn}y_{dn\mathrm{o}3} \\
\lambda_{d1}y_{d1\mathrm{op}} + \lambda_{d2}y_{d2\mathrm{op}} + \lambda_{d3}y_{d3\mathrm{op}} + \lambda_{dn}y_{dn\mathrm{op}} \geq \theta\lambda_{dn}y_{dn\mathrm{op}}
\end{array}\right. \tag{17}$$

$$\left.\begin{array}{l}
\lambda_{d1}x_{d1\mathrm{i}1} + \lambda_{d2}x_{d2\mathrm{i}1} + \lambda_{d3}x_{d3\mathrm{i}1} + \lambda_{dn}x_{dn\mathrm{i}1} \leq \lambda_{dn}x_{dn\mathrm{i}1} \\
\lambda_{d1}x_{d1\mathrm{i}2} + \lambda_{d2}x_{d2\mathrm{i}2} + \lambda_{d3}x_{d3\mathrm{i}2} + \lambda_{dn}x_{dn\mathrm{i}2} \leq \lambda_{dn}x_{dn\mathrm{i}2} \\
\lambda_{d1}x_{d1\mathrm{i}3} + \lambda_{d2}x_{d2\mathrm{i}3} + \lambda_{d3}x_{d3\mathrm{i}3} + \lambda_{dn}x_{dn\mathrm{i}3} \leq \lambda_{dn}x_{dn\mathrm{i}3} \\
\lambda_{d1}x_{d1\mathrm{im}} + \lambda_{d2}x_{d2\mathrm{im}} + \lambda_{d3}x_{d3\mathrm{im}} + \lambda_{dn}x_{dn\mathrm{im}} \leq \lambda_{dn}x_{dn\mathrm{im}}
\end{array}\right\} \tag{18}$$

It is necessary to mention that both the input and output-oriented approaches present the same accuracy when finding the most efficient alternative to select. The simple reason is that outputs are dependent on their fed inputs, i.e., outputs are obtained from inputs. The assessment approach to select depends on what the output represents. A general rule is that the *loss function* should be minimized and the *gain function*should be maximized. For instance, if the output represents a loss function, the input should be minimized, thus input-oriented approach should be adopted. Conversely, if the output quantity represents a gain function, the output-oriented efficiency assessment approach should be adopted. A loss function is a quantity whose increment retards the system's efficiency.

In the efficiency assessment of microgrids $\mathrm{MG}_1$, $\mathrm{MG}_2$, and $\mathrm{MG}_3$, the objective is to optimize the MGs' LOLE by an efficiency-driven optimizer (DEA) and thereafter select the MG with the maximum efficiency. As explained in the input and output orientations, this could be achieved in either of the two methods. Either the outputs are maximized using the DEA output orientation method or the inputs are minimized using the input orientation method. Meanwhile, the output of the MGs' equations (2), (5), and (6) to be optimized is LOLE. Since LOLE is a loss function, i.e., an unwanted quantity that must never be maximized, the input-oriented approach is thus selected to minimize the inputs. Recall that the method is that output orientation maximizes the outputs while the input orientation minimizes the inputs. Subsequently, the input-oriented efficiency assessment approach is adopted to minimize the inputs under a constant return to scale, given the outputs. Compare equations (2), (5), and (6) with a characteristic equation of a straight line shown in (19).

$$LOLE = mL + c \tag{19}$$

where $m$ = slope of the equation, and $c$ = intercept on the vertical (*LOLE*) axis.

To obtain the input and output values, two data points (*Li* and *Lii*) were selected to represent L in each of the straight lines of equations (2), (5), and (6). The points are 10 and 20. The points could be any value provided that they lie on the straight line of the equation. More points can be selected. The more the number of data points, the more the number of DEA input and output fields. This makes the system more robust and increases the accuracy of the resulting system efficiency. Let K represent the number of selected data points. The resulting number of input and output fields for the characteristic multiple linear regression equation is {nK+1} and K, respectively, where n = the number of explanatory variables. However, for simpler analysis, our selected number of data points is limited to two. Hence; the quantities; *mLi*, *mLii*, and *c*; are the inputs while their resulting LOLEs; $LOLE_{Li}$ and $LOLE_{Lii}$; are the outputs. Thus, the respective input and output formats for their DEA efficiency assessment are tabulated in Table 6 (a). Their resulting corresponding values are given in Table 6 (b). For $\mathrm{MG}_1$, equation (20), as shown at the bottom of the next page, is minimized with the constraint in (21), as shown at the bottom of the next page.

Similarly, the efficiencies of $\mathrm{MG}_2$ and $\mathrm{MG}_3$ were also calculated and obtained. It is important to note that the DEA assessment algorithm does not utilize negative values. Meanwhile, in some cases, some of the values could be negative, such as the intercept, C. Hence, the entire values under the data field of the negative value are converted into their non-negative equivalent. Given that $x_i$ is the input vector, $x_j$ is the output vector, and $k$ is the number of data points, the non-negative conversion is achieved using the activation function, *Softmax,*as shown in (22).

$$\mathrm{Softmax}(x_i) = \frac{e^{x_i}}{\sum_{j=1}^{k} e^{x_j}} = \frac{e^{\text{reference datapoint}}}{\text{Summation of } e^{\text{each datapoint}}} \tag{22}$$

**TABLE 6.** DEA Inputs and Outputs of Equations (2), (5), and (6) (a) Data Format (b) Data Values.

(a)

| | INPUTS | | | OUTPUTS | |
|---|---|---|---|---|---|
| **MG** | ***mLi*** | ***mLii*** | ***c*** | $LOLE_{Li}$ | $LOLE_{Lii}$ |
| $MG_1$ | $m_1Li_1$ | $m_1Lii_1$ | $C_1$ | $m_1Li_1+C_1$ | $m_1Lii_1+C_1$ |
| $MG_2$ | $m_2Li_2$ | $m_2Lii_2$ | $C_2$ | $m_2Li_2+C_2$ | $m_2Lii_2+C_2$ |
| $MG_3$ | $m_3Li_3$ | $m_3Lii_3$ | $C_3$ | $m_3Li_3+C_3$ | $m_3Lii_3+C_3$ |

(b)

| | INPUTS | | | OUTPUTS | |
|---|---|---|---|---|---|
| **MG** | ***mLi*** | ***mLii*** | ***c*** | $LOLE_{Li}$ | $LOLE_{Lii}$ |
| $MG_1$ | 458.4 | 916.8 | 5.29 | 463.69 | 922.09 |
| $MG_2$ | 458.19 | 916.38 | 6.1928 | 464.3828 | 922.5728 |
| $MG_3$ | 458.25 | 916.5 | 6.043 | 464.293 | 922.543 |

**TABLE 7.** Input and Output Data for $MG_2$ and $MG_3$.

| | $BCH_2$ | | | $BCH_3$ | | |
|---|---|---|---|---|---|---|
| S/No | $Z_2$ | $N_2$ | $T_2$ | $Z_3$ | $N_3$ | $T_3$ |
| 1 | 862 | 121 | 28.0593 | 855 | 120 | 27.8402 |
| 2 | 1958 | 273 | 63.067 | 379 | 53 | 12.6511 |
| 3 | 1334 | 186 | 43.1465 | 1428 | 199 | 46.1303 |
| 4 | 2172 | 303 | 69.89 | 565 | 79 | 18.5728 |
| 5 | 2250 | 314 | 72.3819 | 248 | 35 | 8.4616 |
| 6 | 245 | 35 | 8.3489 | 1448 | 202 | 46.7627 |
| 7 | 57 | 9 | 2.3638 | 3296 | 459 | 105.786 |
| 8 | 3008 | 419 | 96.586 | 2876 | 401 | 92.3548 |
| 9 | 938 | 131 | 30.5042 | 2749 | 383 | 88.321 |
| 10 | 849 | 119 | 27.6439 | 805 | 113 | 26.2262 |
| 11 | 3574 | 498 | 114.6664 | 1931 | 269 | 62.2041 |
| 12 | 1694 | 236 | 54.6124 | 1001 | 140 | 32.485 |
| 13 | 3005 | 419 | 96.4708 | 628 | 88 | 20.5951 |
| 14 | 1715 | 239 | 55.3084 | 390 | 55 | 12.9959 |
| 15 | 2298 | 320 | 73.9077 | 778 | 109 | 25.3658 |

### *B. BLOCKCHAIN TRANSACTION TIME OPTIMIZATION IN THE ENERGY MARKET*

The transaction time minimization approach is proposed to minimize the time spent in purchasing affordable and backup energy from the prosumers.

#### 1) BLOCKCHAIN TRANSACTION TIME ASSESSMENT

In our paper in [36], the blockchain transaction time assessment was performed. Consequently, the relationship between block size, node size, and transaction time, was obtained. This was achieved by simulating the MG transaction platform using the NS3. In a nutshell, NS3 is an internet-enabled research and educational software for modeling and simulating the occurrences of network discrete events in the real world. The number of trading participants (node size - N), the size of their transactions (block size - Z), and the time taken to complete the transactions (transaction time - T) were given. Consequently, their relationship was obtained as given in (23).

$$T = 0.012Z + 0.1393N + 1.23 \tag{23}$$

Equation (23) is the model equation of $BCH_1$. Similar to the $MG_1$, $MG_2$, and $MG_3$ energy efficiency modeling approach; in section III-A2; the DEA method is utilized to model and compare the transaction timeliness of blockchain transactions considering several blockchain platforms. Thus, two more blockchain platforms were developed from the parent equation (23) and were subsequently modeled. This is to compare their transaction time efficiencies. Consequently, the input and output data of the blockchains, $BCH_2$ and $BCH_3$, were generated as shown in Table 7 using random number seeds, 3 and 4, respectively. The ranges of their input and output data are the same as that of (23). These are given in (24), (25), and (26). That is, equations (24), (25), and (26) are the data intervals of (23), (27), and (28). This implies that data values of Z range from 10 to 3590, N ranges from 2 to 500 and T ranges from 0.8586 to 115.1642.

$$10 \leq Z \leq 3590 \tag{24}$$

$$2 \leq N \leq 500 \tag{25}$$

$$0.8586 \leq T \leq 115.1642 \tag{26}$$

where Z = block size, integer values; N = node size, integer values; and T = transaction time, 4-decimal float values. Following the linear relationship in the data of $BCH_2$ and $BCH_3$, their fitting formulae are obtained as given in (27) and (28) using the least-square linear regression model. Next, their efficiencies are determined and ranked.

$$T_2 = 0.03315034Z_2 - 0.00877778N_2 + 0.54671509 \tag{27}$$

$$T_3 = 0.03488736Z_3 - 0.02125745N_3 + 0.54944503 \tag{28}$$

#### 2) EFFICIENCY ASSESSMENT OF BLOCKCHAIN TRANSACTION TIME

To determine and rank the efficiencies of transaction times of blockchain platforms $BCH_1$, $BCH_2$, and $BCH_3$, the DEA input orientation method is exploited. The objective is to optimize the transaction durations, T, of the blockchains using the efficiency-metric algorithm (DEA). Thereafter, the

$$\text{Min}(\phi) \left| \begin{array}{l} 458.4\,\lambda_{MG_1} + 458.19\,\lambda_{MG_2} + 458.25\,\lambda_{MG_3} \leq \phi_{MG_1}\,458.4\,\lambda_{MG_1} \\ 916.8\lambda_{MG_1} + 916.38\lambda_{MG_2} + 916.5\lambda_{MG_3} \leq \phi_{MG_1}\,916.8\,\lambda_{MG_1} \\ 5.29\lambda_{MG_1} + 6.1928\,\lambda_{MG_2} + 6.043\lambda_{MG_3} \leq \phi_{MG_1} 5.29\lambda_{MG_1} \end{array} \right. \tag{20}$$

$$\left. \begin{array}{l} 463.69\,\lambda_{MG1} + 464.3828\,\lambda_{MG2} + 464.293\,\lambda_{MG3} \geq 463.69\,\lambda_{MG1} \\ 922.09\lambda_{MG1} + 922.5728\lambda_{MG2} + 922.543\lambda_{MG3} \geq 922.09\lambda_{MG1} \end{array} \right\} \tag{21}$$

blockchain with the most efficient transaction time is determined and selected. Considering that the transaction time is a loss quantity that must never be maximized, the blockchain with the most efficient transaction time is defined as that whose inputs (Z & N) are the least minimized given the same level of output (T). Because the transaction time is a loss quantity that must never be maximized, the output orientation method was not selected. To obtain the input and output values, two random points, (*Zi* & *Ni*) and (*Zii* & *Nii*), were selected on each of the trendlines of linear equations (23), (27), and (28). This is similar to the DEA method in the previous section III-A2. The points selected are *Zi*=100, *Ni*=50, *Zii*=1000, and *Nii*=300. Hence; the quantities; *mZi*, *mNi*, *mZii*, *mNii*, and their intercepts, *c*; are the inputs. Their corresponding *T*s; $T_{Zi,Ni}$ and $T_{Zii,Lii}$; are the outputs. Subsequently, the respective input and output formats for the DEA efficiency assessment are tabulated in Table 8 (a). Their resulting values are given in Table 8 (b) and their non-negative equivalent, which is obtained using (22), is presented in Table 8 (c). Since an increment in the output, T, is undesired; T is a loss quantity. Therefore, the input-oriented DEA assessment approach is exploited. For $BCH_1$, equation (29), as shown at the bottom of the page, is minimized with the constraint in (30), as shown at the bottom of the page. The resulting efficiency, $\phi_{BCH1}$, is obtained. Likewise, $\phi_{BCH2}$ and $\phi_{BCH3}$ are calculated and obtained.

The stepwise path to the simulation processes is illustrated in Fig. 8. The left arm examines the supply adequacies of the individual MGs and determines the MG that has the maximum adequacy. The right arm focuses on cost optimization. Its operation is activated at the moment the energy buying cost in the MMG exceeds a set threshold.

Thus, a lower cost is prioritized. Next, the blockchain trading platform whose transaction time is the minimum is determined and selected.

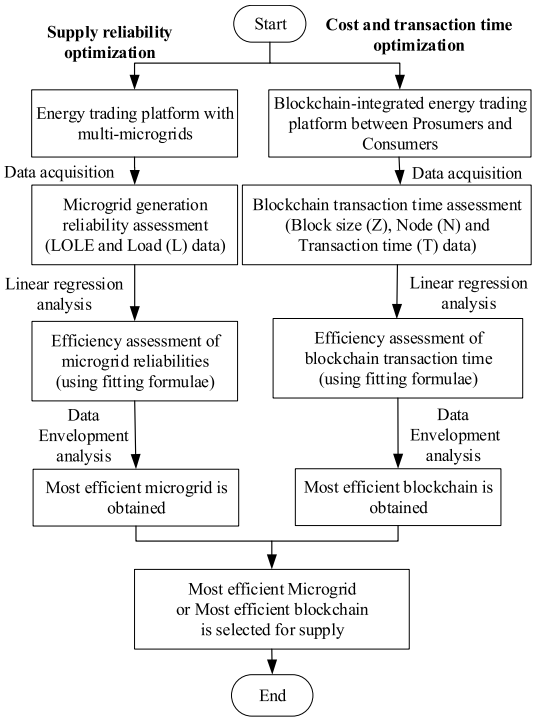


**FIGURE 8.** The stepwise path to the simulation processes.

## IV. RESULTS AND ANALYSIS

### A. EFFICIENCY ASSESSMENT RESULT OF MICROGRIDS' RELIABILITY

From section III-A2, the results of efficiency comparisons of the $MG_1$, $MG_2$, and $MG_3$ are given in Table 9. It was found that the $MG_1$ recorded the maximum power supply efficiency among the three (3) MGs. Considering their model equations (2), (5), and (6), it could appear as if the $MG_1$ would rather have the least efficiency considering that its equation has the maximum slope, 45.84. However, the beauty of the DEA model is that it uses a robust analysis approach. The slopes of the equations are too close in magnitude to make a tangible difference in their effect. The differences in their intercepts are more significant. The DEA model characteristically considers the combined contributions and weights of every input and output feature robustly to reach a decision. The simulation result implies that the $MG_1$ is to be selected for maximum power adequacy supply pending when another MG surpasses it. The MG that surpasses it would then become the new best choice for selection. The efficiency value, 1, of $MG_3$ suggests that its input value, load, is the most minimized to yield the same level of the output, LOLE. Considering a gain function, it offers the best efficiency. However, since the LOLE equation is a loss function, it is regarded as the reverse. Thus, $MG_1$ with the efficiency value, 1.141783, is selected for its least minimized characteristic of the input to yield the same level of output.

$$\text{Min}(\phi) \left| \begin{array}{l} 1.2\,\lambda_{BCH_1} + 3.315034\lambda_{BCH_2} + 3.488736\,\lambda_{BCH_3} \le \phi_{BCH_1}\,1.2\,\lambda_{BCH_1} \\ 12\lambda_{BCH_1} + 33.15034\,\lambda_{BCH_2} + 34.88736\lambda_{BCH_3} \le \phi_{BCH_1}\,12\,\lambda_{BCH_1} \\ 0.999065752\lambda_{BCH_1} + 0.000608311\lambda_{BCH_2} + 0.000325938\lambda_{BCH_3} \le \phi_{BCH_1} 0.999065752\lambda_{BCH_1} \\ \lambda_{BCH_1} + 5.09557E-20\,\lambda_{BCH_2} + 1.20568E-21\,\lambda_{BCH_3} \le \phi_{BCH_1}\,\lambda_{BCH_1} \\ 1.23\lambda_{BCH_1} + 0.54671509\,\lambda_{BCH_2} + 0.54944503\,\lambda_{BCH_3} \le \phi_{BCH_1}\,1.23\lambda_{BCH_1} \end{array} \right. \tag{29}$$

$$\left. \begin{array}{l} 9.395\,\lambda_{BCH_1} + 3.42286\,\lambda_{BCH_2} + 2.975309\,\lambda_{BCH_3} \ge 9.395\,\lambda_{BCH_1} \\ 55.02\,\lambda_{BCH_1} + 31.06372\,\lambda_{BCH_2} + 29.05957\,\lambda_{BCH_3} \ge 29.05957\,\lambda_{BCH_1} \end{array} \right\} \tag{30}$$

**TABLE 8.** DEA Inputs and Outputs of Equations (23), (27), and (28) (a) Data Format, (b) Data, (c) Non-Negative Data.

(a)

| Blockchain | INPUTS | | | | | OUTPUTS | |
|---|---|---|---|---|---|---|---|
| | {Zi , Zii} | | {Ni , Nii} | | | | |
| | ***mZi*** | ***mZii*** | ***mNi*** | ***mNii*** | ***C*** | $T_{Zi,Ni}$ | $T_{Zii,Nii}$ |
| $BCH_1$ | $m_1Zi_1$ | $m_1Zii_1$ | $m_1Ni_1$ | $m_1Nii_1$ | $C_1$ | $m_1Zi_1 + m_1Ni_1 + C_1$ | $m_1Zii_1 + m_1Nii_1 + C_1$ |
| $BCH_2$ | $m_2Zi_2$ | $m_2Zii_2$ | $m_2Ni_2$ | $m_2Nii_2$ | $C_2$ | $m_2Zi_2 + m_2Ni_2 + C_2$ | $m_2Zii_2 + m_2Nii_2 + C_2$ |
| $BCH_3$ | $m_3Zi_3$ | $m_3Zii_3$ | $m_3Ni_3$ | $m_3Nii_3$ | $C_3$ | $m_3Zi_3 + m_3Ni_3 + C_3$ | $m_3Zii_3 + m_3Nii_3 + C_3$ |

(b)

| Blockchain | INPUTS | | | | | OUTPUTS | |
|---|---|---|---|---|---|---|---|
| | {Zi=100 , Zii=1000} | | {Ni=50 , Nii=300} | | | | |
| | ***mZi*** | ***mZii*** | ***mNi*** | ***mNii*** | ***c*** | $T_{Zi,Ni}$ | $T_{Zii,Nii}$ |
| $BCH_1$ | 1.2 | 12 | 6.965 | 41.79 | 1.23 | 9.395 | 55.02 |
| $BCH_2$ | 3.315034 | 33.15034 | -0.43889 | -2.63333 | 0.54671509 | 3.42286 | 31.06372 |
| $BCH_3$ | 3.488736 | 34.88736 | -1.06287 | -6.37724 | 0.54944503 | 2.975309 | 29.05957 |

(c)

| Blockchain | INPUTS | | | | | OUTPUTS | |
|---|---|---|---|---|---|---|---|
| | {Zi=100 ,Zii=1000} | | {Ni=50 , Nii=300} | | | | |
| | ***mZi*** | ***mZii*** | ***mNi (Softmax)*** | ***mNii (Softmax)*** | ***c*** | $T_{Zi,Ni}$ | $T_{Zii,Nii}$ |
| $BCH_1$ | 1.2 | 12 | 0.999065752 | 1 | 1.23 | 9.395 | 55.02 |
| $BCH_2$ | 3.315034 | 33.15034 | 0.000608311 | 5.09557E-20 | 0.54671509 | 3.42286 | 31.06372 |
| $BCH_3$ | 3.488736 | 34.88736 | 0.000325938 | 1.20568E-21 | 0.54944503 | 2.975309 | 29.05957 |

**TABLE 9.** Efficiency Values of Microgrids $MG_1$, $MG_2$, and $MG_3$.

| Microgrid (MG) | Efficiency ($\phi$) |
|---|---|
| $MG_1$ | 1.141783 |
| $MG_2$ | 1.000324 |
| $MG_3$ | 1 |

**TABLE 10.** Efficiency Values of Microgrids $BCH_1$, $BCH_2$, and $BCH_3$.

| Blockchain (BCH) | Efficiency ($\phi$) |
|---|---|
| $BCH_1$ | 7.582534 |
| $BCH_2$ | 1.210702 |
| $BCH_3$ | 1.745928 |

### *B. TRANSACTION TIME EFFICIENCY ASSESSMENT IN THE PROSUMERS' TRADING PLATFORM*

Similarly, in the transaction time efficiency assessment of the blockchain platforms ($BCH_1$, $BCH_2$, and $BCH_3$) in Section III-B2, the obtained results are given in Table 10. Considering a gain function, the $BCH_2$ with an efficiency value of 1.210702 would have been the most efficient choice for being the closest to 1 (Note that the DEA efficiency value of 1 is the most efficient). However, since the transaction time that is being considered is a loss quantity that must never be maximized, the $BCH_1$ with an efficiency of 7.582534 is selected. This is followed by $BCH_3$ and then $BCH_2$. The loss function signifies that the transaction time in Likewise, the selection of the fastest blockchain trading platform is made accordingly pending when another BCH surpasses the current $BCH_2$. The BCH that surpasses it would become the new best choice for selection.

In this paper, the steps of the DEA optimization algorithms as implemented include:

i. The system model equations of the alternatives whose efficiencies are to be compared are developed. For microgrids, the equations are (2), (5), and (6). For blockchains, the equations are (23), (27), and (28).

ii. From the trendline of the equations, the input values are obtained. These are values that lie on the equations' best line of fit. The corresponding outputs are also obtained. For MGs, the input and output values are obtained in Table 6, and for BCHs, they are obtained in Table 8.

iii. The input and output values are then optimized using the parent reference equations (7) and (8). The result of the optimizations is the efficiency values in Tables 9 and 10.

It is helpful to recall that the parent optimization formula (Objective function and constraint) given in (7) and (8) is for the DEA input orientation simulation that was implemented

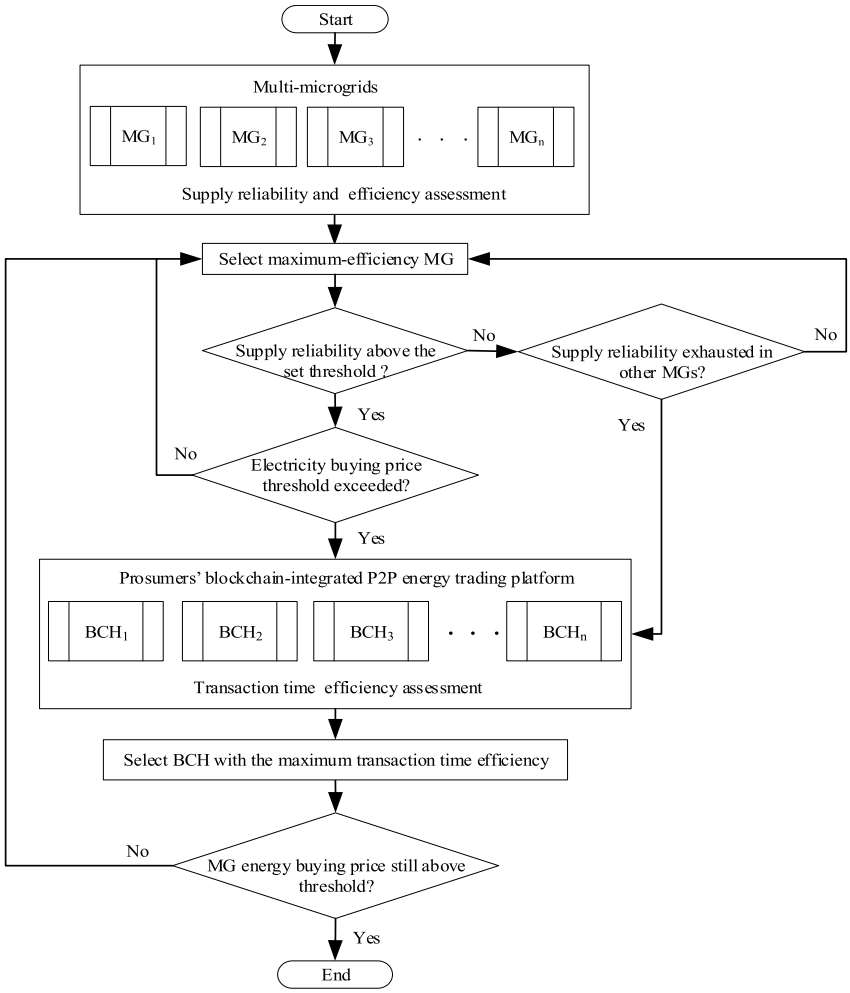


**FIGURE 9.** Consumers' power-switching algorithm.

for each of the MGs and BCHs efficiency simulations. The particular formula that yielded the efficiency value of $MG_1$ of Table 9 are equations (20) and (21) (objective function and its constraint). Similarly, those of $MG_2$ and $MG_3$ were utilized to obtain their efficiency values respectively. The formula that yielded the efficiency value of $BCH_1$ of Table 10 are equations (29) and (30) (Objective function and its constraint). Similarly, efficiency values of $BCH_2$ and $BCH_3$ were obtained. The optimization equations of $BCH_2$ and $BCH_3$ are similar to that of $MG_1$ in (20) and (21) except that the right-hand side bears $MG_2$ or $MG_3$ instead of $MG_1$. They are however omitted to reduce monotony (minimize repetitions). The general format of the optimization equations is given in the "Objective function" equation that is next to (12). It is important to note that in our data simulations, it was assumed that the energy transactions among the participants of the blockchain platforms ($BCH_1$, $BCH_2$, and $BCH_3$) are done randomly as the conditions and needs of the participants warrant. Hence, uninfluenced random data was employed in the modeling of the blockchain transaction. It is also important to note that the scope of study in our manuscript is limited to the standalone generations. For clearer comprehension of the scope, a comparison of the features of this work with other peers is given in Table 11.

**TABLE 11.** Comparison of Features of this Work with the Peers.

| Features | This article | Peer articles |
|---|---|---|
| Collective optimization of energy generation intermittency and transaction latency | ✓ | - |
| Blockchain transaction time optimization with input-oriented DEA | ✓ | - |
| Blockchain transaction time comparison among blockchain peers | ✓ | - |

### C. SWITCHING ALGORITHM BETWEEN MICROGRID AND BLOCKCHAIN TRADING PLATFORM

The blockchain trading platform is preferred and selected under two different conditions:

i. When the reliability of the most efficient MG plummets further than the acceptable limit thereby disconnecting

some consumer loads. This is recorded when the LOLE value of the individual MGs all exceed the acceptable threshold. This is when the supply reliabilities of the individual MGs are all lower than the acceptable threshold. This could occur when RDG generating capacity becomes limited due to low solar irradiation, low wind speed, etc.

ii. When the supply reliabilities are guaranteed but the electricity buying price of all the MGs exceeds the acceptable preset threshold. This mainly occurs during peak consumption hours. Because CDGs are powered at this time, MG operators inflate the electricity buying price to cover the diesel generator operating cost.

The values of the preset thresholds are determined by the consumer at will. The consumers' power-switching algorithm is illustrated in a flowchart in Fig. 9. The maximum-efficiency (most efficient) MG is determined and selected as the consumer's electricity supply source. It is then validated by determining if its supply reliability adheres to the preset threshold (the minimum acceptable reliability). This is the maximum LOLE value that is tolerable considering critical loads. The higher the LOLE value, the lower the MG reliability, and vice versa. Next in the sequence, the electricity buying price is monitored to determine when a set tolerable threshold is exceeded. The supply source is then switched over to the blockchain supply platform whose transaction time efficiency is the maximum. That is, whose transaction time is the shortest. The MGs' electricity buying prices are then monitored and the connection is restored at the moment that the MGs' buying price plummets below the set threshold and with tolerable reliability efficiency.

## V. CONCLUSION

The consumers' consumption satisfaction was considered. Through the energy generation and consumption data in the standalone microgrid, an efficient method to harness the generated energy at maximum adequacy was proposed. In addition, a method was proposed to reduce the transaction delays that are frequently encountered in the trading of the generated energy. These were necessitated by the generation intermittency of standalone MGs as well as the transaction delay bottlenecks in the blockchain-integrated energy transaction platform. Consequently, two specific benefits were achieved. A method to identify and adopt a cost-effective electricity consumption source at maximum adequacy was demonstrated. Also, an approach to achieve a rapid transaction of the traded energies is described and simulated. Finally, an intelligent switching algorithm for optimizing the achieved benefits for consumers is presented. The intelligent switching of consumers' supply sources ensures that electricity supply adequacy is achieved at a more rapid rate and lower buying price. Otherwise, the MGs with deficit generation would conventionally buy electricity from the MGs with surplus generations and sell to the consumers at a higher price. In addition, the delay in doing the energy third-party exchanges is a cost to the critical loads. The overall process ensures maximum penetration of the renewables since MGs with higher reliability are prioritized in the algorithm. This holistically promotes a balance between generation and consumption. However, it is important to mention that the scope of study in our manuscript is limited to the standalone generations. Further study would be focused on how to integrate the intermittency trends of the available generation sources into the existing system to optimize the overall generation efficiency.

## REFERENCES


[1] M. E. T. Souza and L. C. G. Freitas, "Grid-connected and seamless transition modes for microgrids: An overview of control methods, operation elements, and general requirements," *IEEE Access*, vol. 10, pp. 97802–97834, 2022.

[2] M. Cavus, A. Allahham, K. Adhikari, M. Zangiabadi, and D. Giaouris, "Energy management of grid-connected microgrids using an optimal systems approach," *IEEE Access*, vol. 11, pp. 9907–9919, 2023.

[3] Y. Jia, P. Wen, Y. Yan, and L. Huo, "Joint operation and transaction mode of rural multi microgrid and distribution network," *IEEE Access*, vol. 9, pp. 14409–14421, 2021.

[4] F. Fallahi, M. Yildirim, J. Lin, and C. Wang, "Predictive multi-microgrid generation maintenance: Formulation and impact on operations & resilience," *IEEE Trans. Power Syst.*, vol. 36, no. 6, pp. 4979–4991, Nov. 2021.

[5] K.-C. Leung, X. Zhu, H. Ding, and Q. He, "Energy management for renewable microgrid cooperation: Theory and algorithm," *IEEE Access*, vol. 11, pp. 46915–46925, 2023.

[6] E. Quarm, X. Fan, M. Elizondo, and R. Madani, "Proactive posturing of large power grid for mitigating Hurricane impacts," in *Proc. IEEE Power Energy Soc. Innov. Smart Grid Technol. Conf. (ISGT)*, Apr. 2022, pp. 1–5.

[7] J. P. Montoya-Rincon, S. Azad, R. Pokhrel, M. Ghandehari, M. P. Jensen, and J. E. Gonzalez, "On the use of satellite nightlights for power outages prediction," *IEEE Access*, vol. 10, pp. 16729–16739, 2022.

[8] E. Akbari, N. Shafaghatian, F. Zishan, O. D. Montoya, and D. A. Giral-Ramírez, "Optimized two-level control of islanded microgrids to reduce fluctuations," *IEEE Access*, vol. 10, pp. 95824–95838, 2022.

[9] P. J. Colorado, V. P. Suppioni, A. J. S. Filho, M. B. C. Salles, and A. P. Grilo-Pavani, "Security assessment for the islanding transition of microgrids," *IEEE Access*, vol. 10, pp. 17189–17200, 2022.

[10] Z. Liu and L. Wang, "A distributionally robust defender-attacker-defender model for resilience enhancement of power systems against malicious cyberattacks," *IEEE Trans. Power Syst.*, pp. 1–12, 2022.

[11] Y. B. Heng, V. K. Ramachandaramurthy, R. Verayiah, and S. L. Walker, "Developing peer-to-peer (P2P) energy trading model for Malaysia: A review and proposed implementation," *IEEE Access*, vol. 10, pp. 33183–33199, 2022.

[12] M. Touloupou, M. Themistocleous, E. Iosif, and K. Christodoulou, "A systematic literature review toward a blockchain benchmarking framework," *IEEE Access*, vol. 10, pp. 70630–70644, 2022.

[13] B. Li, Z. Pan, and T. Hu, "ReDefender: Detecting reentrancy vulnerabilities in smart contracts automatically," *IEEE Trans. Rel.*, vol. 71, no. 2, pp. 984–999, Jun. 2022.

[14] T. Hu, B. Li, Z. Pan, and C. Qian, "Detect defects of solidity smart contract based on the knowledge graph," *IEEE Trans. Rel.*, Jan. 2023.

[15] M. O. Okoye and H.-M. Kim, "Optimized user-friendly transaction time management in the blockchain distributed energy market," *IEEE Access*, vol. 10, pp. 34731–34742, 2022.

[16] L. Xu, M. Ge, and W. Wu, "Edge server deployment scheme of blockchain in IoVs," *IEEE Trans. Rel.*, vol. 71, no. 1, pp. 500–509, Mar. 2022.

[17] I. Akhtar, M. Jameel, A. Altamimi, and S. Kirmani, "An innovative reliability oriented approach for restructured power system considering the impact of integrating electric vehicles and renewable energy resources," *IEEE Access*, vol. 10, pp. 52358–52376, 2022.

[18] M. O. Okoye, J. Yang, Z. Lei, J. Yuan, H. Ji, H. Wang, J. Feng, T. A. Otitoju, and W. Li, "Predictive reliability assessment of generation system," *Energies*, vol. 13, no. 17, p. 4350, Aug. 2020.

[19] M. O. Okoye and H.-M. Kim, "Adopting the game theory approach in the blockchain-driven pricing optimization of standalone distributed energy generations," *IEEE Access*, vol. 10, pp. 47154–47168, 2022.

[20] A.-D. Nguyen, V.-H. Bui, A. Hussain, D.-H. Nguyen, and H.-M. Kim, "Impact of demand response programs on optimal operation of multi-microgrid system," *Energies*, vol. 11, no. 6, p. 1452, Jun. 2018.
[21] S. Ahmad, M. Shafiullah, C. B. Ahmed, and M. Alowaifeer, "A review of microgrid energy management and control strategies," *IEEE Access*, vol. 11, pp. 21729–21757, 2023.
[22] J. Arshad, M. A. Azad, A. Prince, J. Ali, and T. G. Papaioannou, "REPUTABLE—A decentralized reputation system for blockchain-based ecosystems," *IEEE Access*, vol. 10, pp. 79948–79961, 2022.
[23] Y. Zuo, "Tokenizing renewable energy certificates (RECs)—A blockchain approach for REC issuance and trading," *IEEE Access*, vol. 10, pp. 134477–134490, 2022.
[24] Z. Wang and A. Ben Abdallah, "A robust multi-stage power consumption prediction method in a semi-decentralized network of electric vehicles," *IEEE Access*, vol. 10, pp. 37082–37096, 2022.
[25] S. Verma, D. Yadav, and G. Chandra, "Introduction of formal methods in blockchain consensus mechanism and its associated protocols," *IEEE Access*, vol. 10, pp. 66611–66624, 2022.
[26] J. Yang, J. Dai, H. B. Gooi, H. D. Nguyen, and P. Wang, "Hierarchical blockchain design for distributed control and energy trading within micro-grids," *IEEE Trans. Smart Grid*, vol. 13, no. 4, pp. 3133–3144, Jul. 2022.
[27] W. Liang, Y. Yang, C. Yang, Y. Hu, S. Xie, K.-C. Li, and J. Cao, "PDPChain: A consortium blockchain-based privacy protection scheme for personal data," *IEEE Trans. Rel.*, 2022.
[28] T. M. Masaud, J. Warner, and E. F. El-Saadany, "A blockchain-enabled decentralized energy trading mechanism for islanded networked micro-grids," *IEEE Access*, vol. 8, pp. 211291–211302, 2020.
[29] Ch. V. N. U. B. Murthy, M. L. Shri, S. Kadry, and S. Lim, "Blockchain based cloud computing: Architecture and research challenges," *IEEE Access*, vol. 8, pp. 205190–205205, 2020.
[30] M. Reza Salehizadeh, A. Rahimi-Kian, and M. Oloomi-Buygi, "Security-based multi-objective congestion management for emission reduction in power system," *Int. J. Electr. Power Energy Syst.*, vol. 65, pp. 124–135, Feb. 2015.
[31] S. Jomthanachai, W.-P. Wong, and C.-P. Lim, "An application of data envelopment analysis and machine learning approach to risk management," *IEEE Access*, vol. 9, pp. 85978–85994, 2021.
[32] H. Namvar and S. Bamdad, "Efficiency assessment of resilience engineering in process industries using data envelopment analysis based on type-2 fuzzy sets," *IEEE Access*, vol. 9, pp. 883–895, 2021.
[33] C.-N. Wang, N.-A.-T. Nguyen, T.-T. Dang, and J. Bayer, "A two-stage multiple criteria decision making for site selection of solar photovoltaic (PV) power plant: A case study in Taiwan," *IEEE Access*, vol. 9, pp. 75509–75525, 2021.
[34] M. U. I. Alahakoon and S. N. Jehan, "Efficiency of public service delivery—A post-ICT deployment analysis," *Economies*, vol. 8, no. 4, p. 97, Nov. 2020.
[35] M. R. Salehizadeh, A. Rahimi-Kian, and M. Oloomi-Buygi, "A multi-attribute congestion-driven approach for evaluation of power generation plans," *Int. Trans. Electr. Energy Syst.*, vol. 25, no. 3, pp. 482–497, Mar. 2015.
[36] M. Onyeka Okoye, J. Yang, J. Cui, Z. Lei, J. Yuan, H. Wang, H. Ji, J. Feng, and C. Ezeh, "A blockchain-enhanced transaction model for microgrid energy trading," *IEEE Access*, vol. 8, pp. 143777–143786, 2020.

**MARTIN ONYEKA OKOYE** received the B.Eng. degree in electrical/electronics and computer engineering from Nnamdi Azikiwe University, Awka, Nigeria, in 2008, the M.Sc. degree in electronic systems design engineering from Universiti Sains Malaysia, Penang, Malaysia, in 2018, and the Ph.D. degree in electrical engineering from the Shenyang University of Technology, Shenyang, China, in 2021. He was a Postdoctoral Researcher with the Department of Electrical Engineering, Incheon National University, Incheon, South Korea, until December 2022. He is currently a Profesor Asociado with the Department of Electrical Engineering, Pontificia Universidad Católica de Valparaíso, Chile. His research interests include generation system reliability assessment, blockchain technology, distributed renewable generations, and microgrid operation.

**GONZALO FARÍAS CASTRO** received the degree in computer science from the University of La Frontera, Temuco, Chile, in 2001, and the Ph.D. degree in automatic and system engineering from the National University of Distance Education, Madrid, Spain, in 2010. Since 2012, he has been with the School of Electrical Engineering, Pontificia Universidad Católica de Valparaíso, Valparaíso, Chile. His current research interests include pattern recognition and machine learning and the simulation and control of dynamic systems.

**SEBASTIÁN FINGERHUTH** (Member, IEEE) received the bachelor's degree (E.Eng.) from Pontificia Universidad Católica de Chile (PUC), in 2003, and the Ph.D. degree (Dr.-Ing.) in acoustics from RWTH Aachen University, Germany, in 2009. He was a Math and Physics Teacher with PUC. As a Researcher and an Engineer, he worked in acoustic, psychoacoustic, vibrations, and noise reduction projects with RWTH Aachen University, Germany. He is currently a full-time Professor with the School of Electrical Engineering, Pontificia Universidad Católica de Valparaíso. He is working in projects in areas, such as acoustics, structural vibration, instrumentation, sensors, and signal processing. He is a member of the German Acoustic Society (DEGA) and the American Society of Acoustics (ASA).

**JUNYOU YANG** received the B.Eng. degree from the Jilin University of Technology, Jilin, China, the M.Sc. degree from the Shenyang University of Technology, Shenyang, China, and the Ph.D. degree from the Harbin Institute of Technology, Harbin, China. He was a Visiting Scholar with the Department of Electrical Engineering and Computer Science, University of Toronto, Canada, from 1999 to 2000. He is currently the Head of the School of Electrical Engineering, Shenyang University of Technology. He is also a Distinguished Professor of Liaoning province and the first 100 level candidates with the BaiQianWan Talents Program. He has led more than 50 research projects and has more than 200 publications in his technical field. His research interests include wind energy, special motor, and its control.